International Journal of Automotive Technology, Vol. 7, No. 2, pp. 145–154 (2006)

1229-9138/2006/026-04

DEVELOPMENT OF MATDYMO (MULTI-AGENT FOR TRAFFIC SIMULATION WITH VEHICLE DYNAMICS MODEL) II: DEVELOPMENT OF VEHICLE AND DRIVER AGENT

K.-Y. CHO[1], S.-J. KWON[1] and M.-W. SUH[2]*

[1]Graduate School of Mechanical Engineering, Sungkyunkwan University, Geonggi 440-746, Korea
[2]School of Mechanical Engineering, Sungkyunkwan University, Geonggi 440-746, Korea

(Received 4 March 2005; Revised 31 August 2005)

ABSTRACT–In the companion paper, the composition and structure of the MATDYMO (Multi-Agent for Traffic Simulation with Vehicle Dynamic Model) were proposed. MATDYMO consists of the road management system, the vehicle motion control system, the driver management system, and the integration control system. Among these systems, the road management system and the integration control system were discussed In the companion paper. In this paper, the vehicle motion control system and the driver management system are discussed. The driver management system constructs the driver agent capable of having different driving styles ranging from slow and careful driving to fast and aggressive driving through the yielding index and passing index. According to these indices, the agents pass or yield their lane for other vehicles; the driver management system constructs the vehicle agents capable of representing the physical vehicle itself. A vehicle agent shows its behavior according to its dynamic characteristics. The vehicle agent contains the nonlinear subcomponents of engine, torque converter, automatic transmission, and wheels. The simulation is conducted for an interrupted flow model and its results are verified by comparison with the results from a commercial software, TRANSYT-7F. The interrupted flow model simulation is implemented for three cases. The first case analyzes the agents' behaviors in the interrupted flow model and it confirms that the agent's behavior could characterize the diversity of human behavior and vehicle well through every rule and communication frameworks. The second case analyzes the traffic signals changed at different intervals and as the acceleration rate changed. The third case analyzes the effects of the traffic signals and traffic volume. The results of these analyses showed that the change of the traffic state was closely related with the vehicle acceleration rate, traffic volume, and the traffic signal interval between intersections. These simulations confirmed that MATDYMO can represent the real traffic condition of the interrupted flow model. At the current stage of development, MATDYMO shows great promise and has significant implications on future traffic state forecasting research.

KEY WORDS : Vehicle dynamics, Multi-agent, Traffic simulation, Virtual driving lane, Interrupted flow model, Uninterrupted flow model

1. INTRODUCTION

Traffic can be viewed as a complex system (Helbing and Schreckenberg, 1999). Traffic simulation models are typically classified as a micro model and macro model. As one of the primary approaches to modeling complex systems, macro models focus on the observable behavior of a system. Macro models define and regenerate the observable behavior of a system in terms of aggregates and their probability distributions. For traffic, macro models are usually derived from fluid dynamics, and they involve aggregate parameters such as traffic volume and average speed on artilleries in a traffic network.

Simulations using macro models are advantageous in that run-time can be fairly short. Macroscopic models are sufficient for obtaining a coarse prediction of conditions. However, most complex systems are highly nonlinear and often extremely sensitive to initial conditions. Even infinitesimal perturbations to initial conditions can have an arbitrarily large impact on the global system behavior. In the process of aggregating and abstracting information, macro models often lose their sensitivity.

Micro modeling is another approach that can perform better macro modeling. Micro models treat a system as a large set of small, interacting components. They focus mainly on identifying the components in a system, discovering their local behaviors, and understanding their

*Corresponding author. e-mail: suhmw@yurim.skku.ac.kr

interactions. Global system behavior emerges from the local behaviors and interactions of individual components. As reported in many articles in a wide range of domains (Reynolds, 1987; Mataric, 1994), very complex and realistic global behavior can be obtained from simple local behaviors. For traffic, micro models have focused on driver behavior, car following, and lane changing models.

In micro simulation, the main issues are computational performance and software development cost. Micro simulations emulate the behavior of every individual entity in the system, and thus, they are computation intensive. Running a micro simulation of a metropolitan area traffic network involves the behaviors of millions of cars, traffic signals, etc, so the simulation can be very time consuming. Conventional software design and implementation principles and tools do not readily provide the support to define local behaviors and interactions of entities in a micro simulation (Wenpin and Hong, 2004). Therefore, a new software paradigm was required.

Advances in distributed control and computer networks have culminated in the agent technology, a natural successor to the object-oriented paradigm. A multi agent system consists of autonomous objects (agents) that encapsulate not only local information and algorithmic expertise, but also local control and self-initiative. Agents interact by exchanging information, and the global system behavior emerges from their interactions. In recent years, a number of agent infrastructures with varying flavors and sophistication have been developed to facilitate the implementation of multi-agent systems. Although multi agent-based approach has many advantages, it has difficulty in sufficiently accounting for the traffic-affecting elements such as the characteristics of each individual driver and vehicle, etc.

The companion paper (Cho *et al.*, 2005) presented our approach for building a multi-agent system in the traffic simulation, that is, the MATDYMO (Multi-Agent for Traffic Simulation with Vehicle Dynamic Model). The requirements of the traffic simulation were analyzed and the configuration of MATDYMO was discussed. The MATDYMO has four main systems, the road management system, the vehicle motion control system, the driver management system, and the integration control system. Among these systems, the road management system and the integration control system were discussed in companion paper. In this paper, the vehicle motion control system and the driver management system are discussed.

2. DRIVER MANAGEMENT SYSTEM

In this chapter, we discuss the driver management system which constructs the driver agent. The driver management system consists of the path finding module, the car following module, and the lane changing module. It sends the desired acceleration derived from the car following module to the vehicle motion control system. Also, it transfers the vehicle motion information to the road management system and the integration control system.

2.1. Path Finding Module

Path selection autonomy is one of the most important characteristics that represent the diversity of a driver. For example, although the drivers have a same departure and destination, they may choose different paths according to their experience and preference. All drivers do not choose the shortest path with respect to the travel time or the total distance. The ideal path finding method would search every possible path. But if the road network size is increased, the computational cost may increases by geometric progression (Jones, 1993). Therefore, a path finding algorithm which can search the optimal path efficiently and express the diversity of the driver is needed. In this paper, we use A* algorithm (Kuri *et al.*, 2002) to find the optimal path. The utility function, u, is shown as follows. The optimal path is the path that maximizes the utility function.

$$u = \sum_{i}^{M} w_i s_i \tag{1}$$

where M is a number of factors defined over solutions, w is a parameter controlling the impact of penalties, s is a candidate solution, and subscription i is the considering factor. The road cost, c, is defined as follows.

$$c = \frac{1}{u} \tag{2}$$

In equation (2), the maximization of the utility function means the minimization of the cost. Hence, the problem is to find a path at minimum cost. The factors considered in this study are the traveling cost, the traveling time, and the degree of path complexity. The evaluation function, $f(n)$, is defined as equation (3).

$$f(n) = g(n)+h(n) \tag{3}$$

where, $g(n)$ is the cost of node n from the start state and $h(n)$ means the heuristic estimation of the cost from n to a goal. The heuristic function, $h(n)$, is defined as below.

$$h(n) = a_1 l + a_2 \frac{l}{V_{\max}} \tag{4}$$

where l is the length between the node n and the goal, $V_{\max}$ is the maximum velocity of average velocities of all roads, and a is weight function. Therefore, the following inequalities are satisfied.

$$x_1 \geq l \tag{5}$$

$$x_2 \geq \frac{l}{V_{\max}} \tag{6}$$

where x is the features of a particular position, Generally, if the inequality equation, $h^*(n)-h(n) \geq 0$, is satisfied, the optimal path can be found at minimum cost by the A* algorithm (Jones, 1993). Here, $h^*(n)$ is the real cost from node n to the goal node.

$$h^*(n)-h(n) = a_1(x_1 - l)+a_2\left(x_2 - \frac{l}{V_{\max}}\right) \geq 0 \tag{7}$$

2.2. Efficiency of the Path Finding Module

In this section, A* algorithm is compared with other algorithms such as the breadth first search and bi-directional search. To verify the path finding module, the road around Sungkyunkwan University presented in Figure 1 was chosen as a sample road network. The total nodes number was 58, and the value of the branching factor was 2.51. The calculation result of route search for the sample road network is shown in Table 1. Because the effective branching factor (b*) is around 1.3, A* algorithm is available. Generally the number of expanded nodes, N, of A* algorithm is defined as follows.

$$N = \sum_{k=1}^{d} (b^*)^k \tag{8}$$

where, d means the depth of the solution. The number of expanded nodes of the breadth first search and bi-directional search are defined as follows.

$$N = \sum_{k=1}^{d} b^k \tag{9}$$

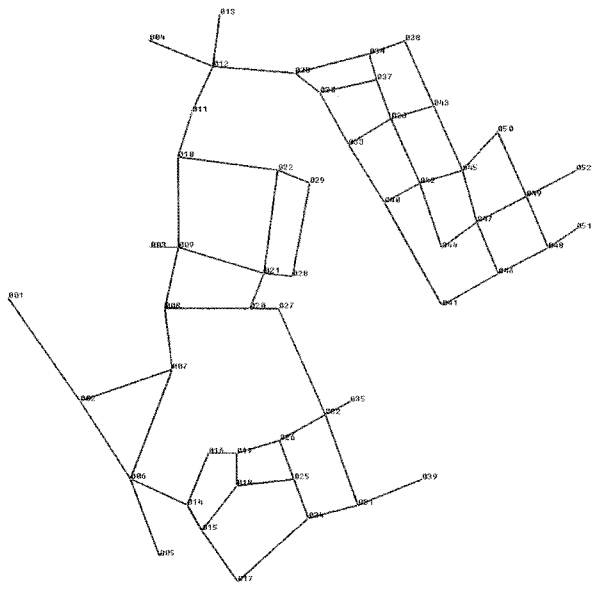

Figure 1. Road network around Sungkyunkwan Univ..

Table 1. Result of calculation.

	d	N	b*
a_1=1	7	21	1.278
a_1=1, a_2=1	8	21	1.213
a_1=1, a_3=1	8	33	1.314

$$N = \sum_{k=1}^{d/2} b^k \tag{10}$$

here, d and b* are the number of links from the origin to the destination. And b is the branching factor, which is 2.51 in this example. For the depth of solution, A* algorithm can calculate a problem that is 1.8 times~2.5 times larger than other problems. For the same number of nodes, the search cost ratio of the breadth first search to A* algorithm is $(b/b^*)^n$. And the search cost ratio of A* algorithm to bi-directional search is derived as $(\sqrt{b}/b^*)^n$. Hence, A* algorithm was suitable as a path finding algorithm. The search cost and branching factors for each case are shown in Figure 2.

2.3. Car Following Module

The car following module has two basic function modes: the speed limit control and the follow control (Venhovens *et al.*, 2000). With no leading vehicle detected within the visible range, the vehicle is controlled according to the speed limit of the road through the speed limit control. But, if there is a preceding vehicle, the vehicle follows the leading vehicle in the following control mode. The algorithm of the car following module is based on the assumption described by the following equation (Nakamiti and Freitas, 2002).

$$x_{i-1}(t + T)-x_i(t + T) = D_i(t + T) \tag{11}$$

where, $x_i(t)$ is the position and $D_i(t)$ is the desired distance of vehicle i at time t to vehicle i-1. Also, we assumed the

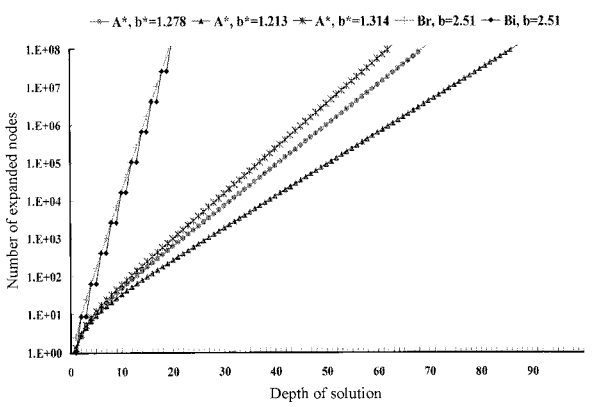

Figure 2. Comparison of the search costs and branching factors.

desired distance as a quartic function of the speed within the urban range in this paper. It is described as equation (13).

$$D_i = \alpha v_i^4 + \beta \tag{12}$$

where, v_i is the speed of vehicle i, α is 0.000161, and β is 1.0.

2.3.1. Limit speed control algorithm

If the preceding vehicle is moving beyond the desired distance, the speed limit control makes the following vehicle maintain the speed limit of the road. As shown in Figure 3, the error between the desired distance of the speed limit and the actual distance from the measured speed is derived by equation (14) (Fujioka and Suzuki, 1994). The sliding face for the error is determined by equation (15), and the sliding controller is derived as the equation (16). Therefore, the desired acceleration for the speed limit control is presented in equation (17).

$$\begin{aligned} \varepsilon_1 &= x_{r\_limit\_des} - x_{r\_des} \\ &= v_{limit\_speed} \cdot h - v_F \cdot h \end{aligned} \tag{13}$$

$$S_1(x;t) = \varepsilon_1 + w_1 \int \varepsilon_1 dt \tag{14}$$

$$\dot{S}_1(t) = -c_1 S_1(t) \tag{15}$$

$$a_{f\_des} = \frac{c_1 S_1 + w_1 \varepsilon_1}{h} \tag{16}$$

where, $x_{r\_limit\_des}$ is the desired distance, x_{r_set} is the actual desired distance, v_{limit_speed} is the speed limit, v_F is the speed of the Subject Vehicle and c_1, w_1 are the control constants.

2.3.2. Follow control

When the subject vehicle follows the leading vehicle, as shown in Figure 4, the error between the desired distance and relational distance measured by sensors, is expressed

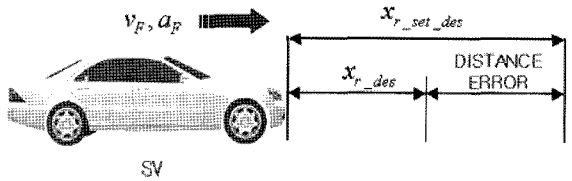

Figure 3. Overview of the limit speed control algorithm.

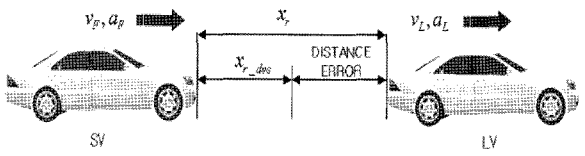

Figure 4. Overview of the follow control algorithm.

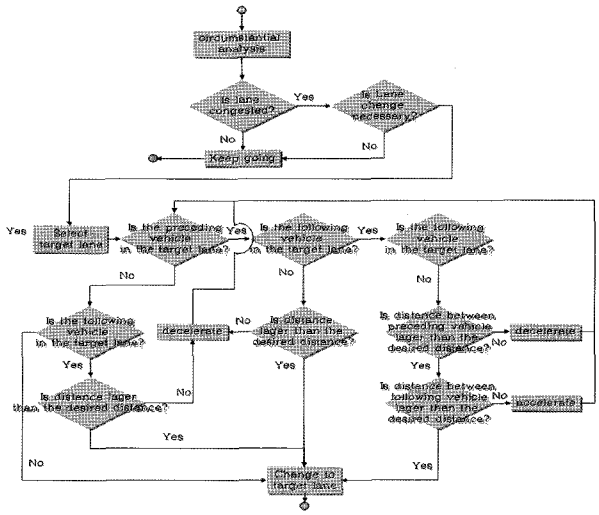

Figure 5. Flow chart of the dynamic lane changing process in the MATDYMO.

by equation (18). The sliding face for the error is determined by equation (19), and the sliding controller is formed as the equation (20). Also, the desired acceleration is expressed by equation (21).

$$\varepsilon_2 = x_r - x_{r\_des} = x_r - v_F \cdot h \tag{17}$$

$$S_2(x;t) = \varepsilon_2 + w_2 \int \varepsilon_2 dt \tag{18}$$

$$\dot{S}_2(t) = -c_2 S_2(t) \tag{19}$$

$$a_{f\_des} = \frac{c_2 S_2 + w_2 \varepsilon_2 + v_L - v_F}{h} \tag{20}$$

2.4. Lane Changing Module

In this paper, the lane changing maneuvers are classified into two types: static and dynamic. Static lane changing occurs not by the interface of neighboring vehicles but by the interface of the driving paths. On the other hand, dynamic lane changing occurs by the interaction with adjacent agents through complex decision-making processes.

2.4.1. Static lane changing module

The static lane changing maneuvers occur when vehicles follow their path, planned initially. That is, to go left or right, vehicles change their lane to the neighboring lane which is possible to turn left or right. Hence, static lane changing plan is determined at the time of vehicle generation.

2.4.2. Dynamic lane changing module

Dynamic lane changing maneuvers occur in a congested road situation. That is, in order to avoid the traffic congestion, vehicles change their lane to the neighboring

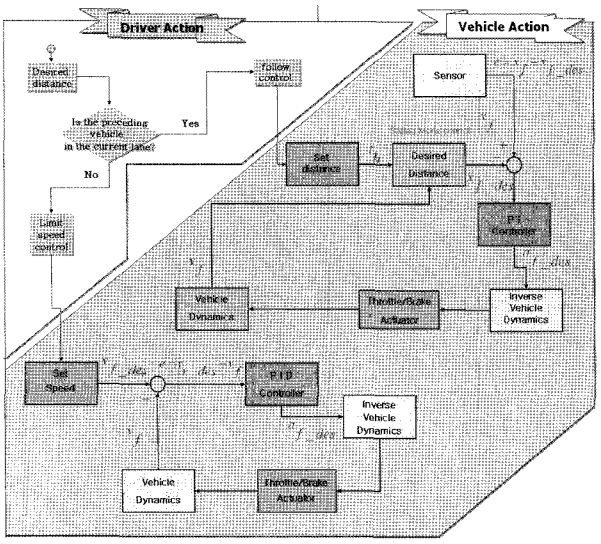

Figure 6. Relation of the driver agent and the vehicle agent.

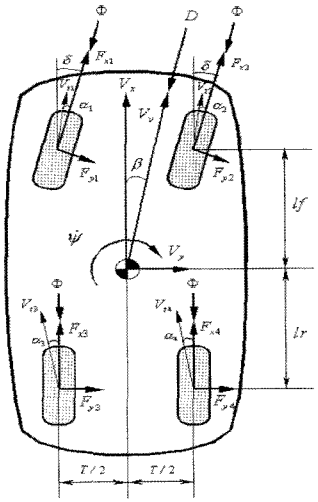

Figure 7. Vehicle dynamics model for the MATDYMO system.

lane. Hence, dynamic lane changing is determined by the traffic conditions and the characteristics of the driver agent. The factors that affect dynamic lane changing are "yielding index" and "passing index". These indices are discussed In the companion paper. The flow chart of dynamic lane changing is shown in Figure 5.

3. VEHICLE MOTION CONTROL SYSTEM

The vehicle motion control system constructs the vehicle agent, which is the vehicle itself, composed of the vehicle model and controllers. Also, the vehicle agent contains the physical attributes of the vehicle such as length, acceleration rate, type, etc. The relation of the driver agent and the vehicle agent is shown in Figure 6. To consider vehicle dynamics, we constructed the vehicle model having 8 DOF (Degrees-Of-Freedom). The vehicle motion control system consists of the vehicle dynamics control module, throttle control module, and brake control module. The driver agent analyses the traffic condition, computes the desired acceleration, and sends the desired acceleration to the vehicle agent. The vehicle agent calculates the real acceleration according to the vehicle characteristics and sends it back to the driver agent.

3.1. Vehicle Dynamics Control Module

To analyze the dynamic characteristics of a vehicle, the equations of motion describe the longitudinal motion, the lateral motion, the yawing motion, and the rotational motion of wheels, respectively. The suspension system is ignored, and the mathematic vehicle model is shown in Figure 7 (Kwon *et al.*, 2004). The equations of longitudinal, lateral, and yawing motion are presented below.

• the longitudinal motion

$$\begin{aligned} M(V_x - V_y\dot{\theta}) = {} & F_{x1}\cdot\cos\delta - F_{y1}\cdot\sin\delta \\ & F_{x2}\cdot\cos\delta - F_{y2}\cdot\sin\delta + F_{x3} + F_{x4} \end{aligned} \tag{21}$$

where, V_x is the longitudinal velocity, and V_y, $\dot{\theta}$ are the lateral velocity and the yawing velocity, and M, δ are the mass and angular displacement, respectively.

Subscript x and subscript y denote x direction and y direction, respectively. F_{x_i} and F_{y_i} are the applied forces calculated in the tire i in the longitudinal direction.

• the lateral motion

$$\begin{aligned} M(\dot{V}_y + V_x\dot{\theta}) = {} & F_{x1}\cdot\sin\delta + F_{y1}\cdot\cos\delta \\ & + F_{x2}\cdot\sin\delta + F_{y2}\cdot\cos\delta + F_{y3} + F_{y4} \end{aligned} \tag{22}$$

• the yawing motion

$$I_z\ddot{\theta} = F_{T1} + F_{T2} + F_{T3} + F_{T4} \tag{23}$$

where, I_z is the mass moment of inertia in the z direction, F_T is the yawing moment on the body due to the applied force in the tires, and moments F_{T1}, F_{T2}, F_{T3}, F_{T4} are defined as follows:

$$\begin{aligned} F_{T1} = {} & a\cdot(F_{x1}\cdot\sin\delta + F_{y1}\cdot\cos\delta) \\ & + \frac{T}{2}(F_{x1}\cdot\cos\delta - F_{y1}\cdot\sin\delta) \end{aligned}$$

$$\begin{aligned} F_{T2} = {} & a\cdot(F_{x2}\cdot\sin\delta + F_{y2}\cdot\cos\delta) \\ & + \frac{T}{2}(F_{x2}\cdot\cos\delta - F_{y2}\cdot\sin\delta) \end{aligned}$$

$$F_{T3} = -b \cdot F_{y3} + \frac{T}{2} \cdot F_{x3}$$
$$F_{T4} = -b \cdot F_{y4} - \frac{T}{2} \cdot F_{x4} \quad (24)$$

where, T is the width of the vehicle, a, b are the length between the front wheel and center of gravity and the length between the real wheel and center of gravity, respectively.

The longitudinal vehicle model is used in simulation studies to describe the behavior of an actual vehicle. The six sub components of the longitudinal vehicle model are the engine, torque converter, transmission, drive train, throttle, and brake actuator. The external inputs to the longitudinal vehicle model are the throttle angle and brake torque. The primary output is the vehicle speed. The engine model determines the engine torque from the air mass flow inhaled through the throttle valve. The engine torque determined by the engine model generates the tractive torque needed by a vehicle to accelerate. The engine torque shown in Figure 8 is determined by the throttle ratio and RPM.

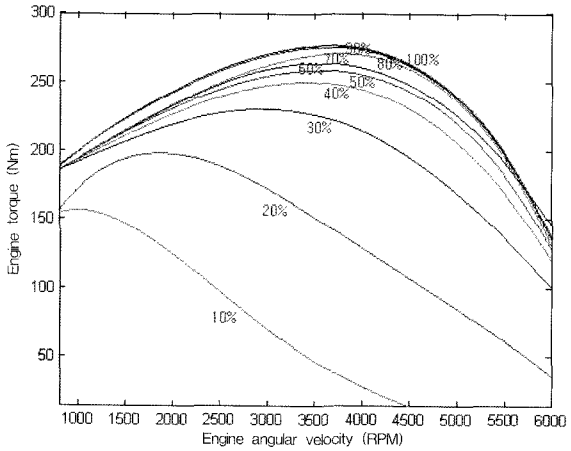

Figure 8. Engine map.

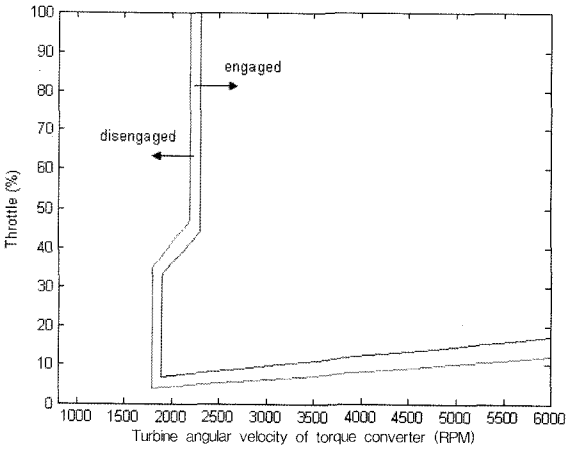

Figure 9. Lock-Up map.

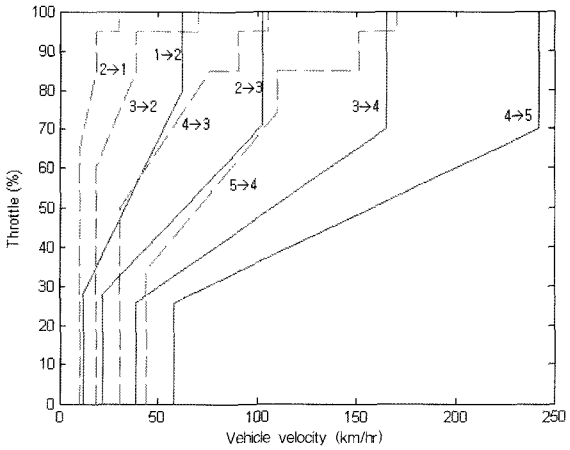

Figure 10. Gear shift map.

In the torque converter model, the turbine torque is calculated by multiplying the engine torque according to the torque ratio. The torque ratio is a nonlinear function of the speed ratio, which is the ratio of the turbine speed to the engine speed. In this study, the lock-up map of the torque converter which engages the pump-side rotational frequency to be same as the turbine-side rotational frequency is represented as the lookup tables of Figure 9. The transmission model determines gear shifting based on the vehicle speed and throttle ratio. The throttle shift point is determined based on the current vehicle speed and the throttle ratio when it is time to shift. Figures 10 shows the gear shift map. Also, the delay time in the throttle and brake actuator is assumed as zero.

3.2. Throttle Control Module

An inverse vehicle dynamic model is used to control the throttle for the desired acceleration. As shown in figure 11, the desired engine torque is derived by the desired acceleration, and then the throttle ratio is derived from desired engine torque by using the inverse engine map.

Using the inverse vehicle dynamic model, the desired engine torque and the engine speed are derived from the desired acceleration in the previous chapter from equations (25) and (26). These values are used as input factors in the inverse engine map, and the required throttle ratio can be obtained.

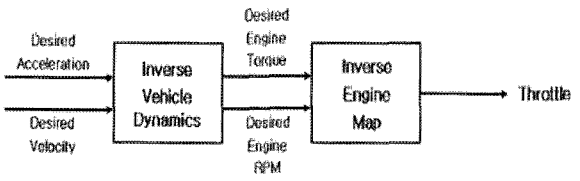

Figure 11. Throttle control module.

$$T_{E\_des} = \frac{r(m \cdot a_{f\_des} + F_D)}{N_t N_f} \quad (25)$$

$$\omega_e = \frac{v_F \cdot N_F \cdot N_f}{R} \quad (26)$$

where m is the mass of the vehicle, and r is the tire radius, F_D is the road load, N_t is the numerical ratio of the transmission, N_f is the numerical ratio of the final drive, T_{E_des} is the desired engine torque and ω_e is the rotational speed of the engine.

3.3. Brake Control Module

The desired brake pressure can be shown by the expression, the equation (27).

$$P_{b\_des} = \frac{1}{K_b}\{-R(Ma_{f\_des} + F_D)\} \quad (27)$$

where K_b is the brake gain, and P_{b_des} is the desired brake pressure.

4. ROAD NETWORK SIMULATION

MATDYMO was evaluated via simulation to identify its properties and possible weaknesses for a variety of scenarios and cases. First, the vehicle agent behaviors in the microscopic aspect have been analyzed in the interrupted flow model. Second, the traffic flow was analyzed by using the interval of the traffic signals and acceleration rate in the interrupted flow model. Third, traffic flow considering the interval of the traffic signals and traffic volume was analyzed.

4.1. Analysis of the Agent Behaviors in the Interrupted Flow Model

The congested and interrupted flow model was simulated, as shown in Figure 12. The interrupted flow model, which does not contain an equilibrium speed-density relationship, showed the road in the state of discontinuous traffic flow like an urban way. The model was simulated for 1 hour and the time step was 1 ms. The road speed limit was 60 km/h and the applied congestion density was 120 vehicles/km. The ratio of the turning

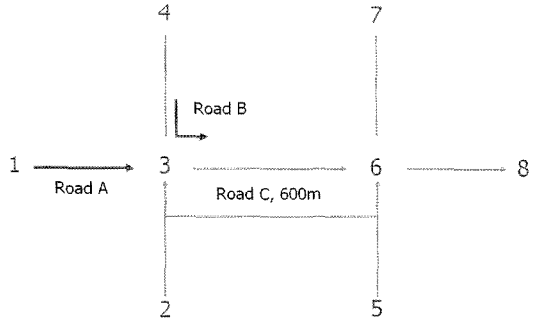

Figure 12. Condition of the road network for simulation.

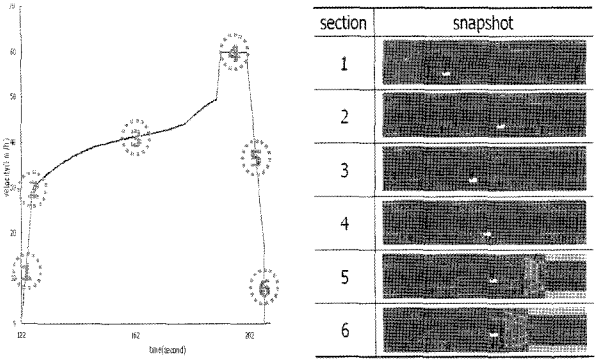

Figure 13. Velocity profile and snapshots of the vehicle A from 120 s to 220 s.

Table 2. Conditions of the signal.

Node \ Signal	Green (s)	Orange (s)	Red (s)	Period (s)
3, 6	35	2	38	75

traffic volume to the straight one was 25% at node 3. Vehicles were generated at nodes 1 and 4, and terminated at node 8. The traffic signals were located at node 3 and 6. The conditions of the traffic signals are shown in Table 3.

The length of road C was 600m. The applied vehicle acceleration rate ranged from -3 m/s^2~2.0 m/s^2. The average traffic volume (V/C) was 0.71 in this simulation. The vehicle-color pairs used were as follows: the target vehicle 1-white and the other vehicles-red. In this simulation, vehicle behaviors such as changing lane, speeding up/down, passing, and following others, were achieved to analyze the interactive effect to adjacent vehicles. The movement of vehicle 1, V1, was presented as continuous images with the velocity profile by simulation times in the Figure 13. Vehicle A was generated at node 4 and terminated at node 8: the route of V1 was node 4368. Vehicle 1 sped up by the speed limit control at the initial time and V1. V1 found another vehicle at the same lane and slowed down until it reached the desired relative distance. After that, V1 followed another vehicle by the follow control. At the intersection, V1 traveled according to the traffic signals. After passing the intersection, V1 changed its lane dynamically to avoid the traffic congestion. The total velocity profile of V1 is

Table 3. Characteristics of vehicles.

Type	Acceleration rate (m/s^2)
A	-3 m/s^2~2.0 m/s^2
B	-2.89 m/s^2~2.89 m/s^2

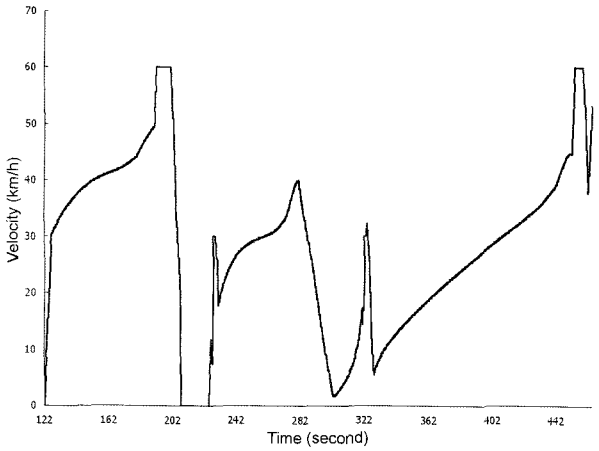

Figure 14. Velocity profile of vehicle A.

shown in Figure 14. The velocity profile shows the flexible movement according to the speed limit control and following control. Vehicles are substantially affected by adjacent vehicles and, in turn, affect the velocity of the traffic as a whole.

4.2. The Effects of Traffic Signals Interval and Acceleration rate

The same road shape and traffic signal condition in section 4.1 was used to analyze the traffic flow according to the interval of the traffic signals and the acceleration rate. Nodes in which vehicles are generated and terminated are the same as the above simulation.

The period of simulation was 1 hour and the time step is 1 ms. A speed limit was 60 km/h and a congestion density was 120 vehicles/km. Also, the saturation traffic volume (V/C) was 2400 vehicles/h. The ratio of turning traffic volume to straight one was 25% at node 3. In this simulation, the average delay of road C between node 3 and 6 was observed. The average traffic volume was 0.71. The two kinds of acceleration rate were applied as shown in Table 4. The first applied acceleration rate ranged from -3 m/s^2~2.0 m/s^2 proposed by ISO/TC2004 as the acceleration rate of ACC (Adaptive Cruse Control) international standard (ISO 15622, 2002). Another rate ranged from -2.89 m/s^2~2.89 m/s^2 proposed by Go (Ben-Akiva *et al.*, 1985) as the empirical acceleration rate. The results were compared with those from a commercial software, TRANSYT-7F (T7F, Lin and Gan, 1999). The MATDYMO showed very similar result to T7F for various acceleration rates. The maximum and minimum of the average delay at MATDYMO changed by the acceleration rate similar to those of T7F. That is, the optimum state of traffic signals was affected by the acceleration rate. The result showed that the larger the acceleration rate, the more sensitive the variation of average delay. The minimum average delay resulted at

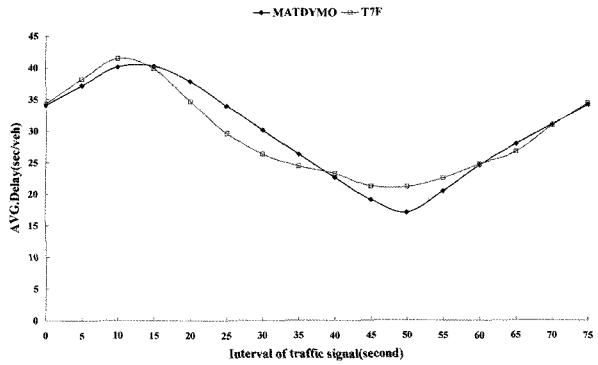

Figure 15. Variation of the average density by the interval of the traffic signals at type A.

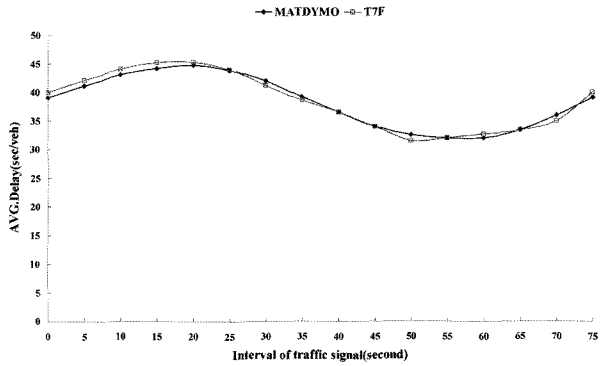

Figure 16. Variation of the average density by the interval of the traffic signals at type B.

the larger acceleration rate. Because the input traffic volume was constant, the passing traffic volume per unit volume was constant, the passing traffic volume per unit time increased at higher acceleration rate. Therefore, because the passing traffic volume was large, the average delay was changed sensitively by the acceleration rate. For this reason, to maintain a smooth traffic flow, the traffic signals for the road network have to be controlled by the acceleration rates of the passing vehicles. Variation of the average density by the interval of the traffic signals are shown in Figures 15 and 16.

4.3. The Effects of the Interval of the Traffic Signals and the Traffic Volume

The same shape and traffic signals condition in section 4.1 was used to analyze the traffic flow according to the interval of the traffic signals and the changing the traffic volume (V/C) at road C in Figure 12. The nodes at which vehicles were generated and terminated were the same as those in the above simulation. The period of simulation was 1 hour and the time step is 1 ms. The speed limit was 80 km/h and a congestion density was 120 vehicles/km. Also, the saturation traffic volume was 2400 vehicles/h. The ratio of turning traffic volume to straight one was

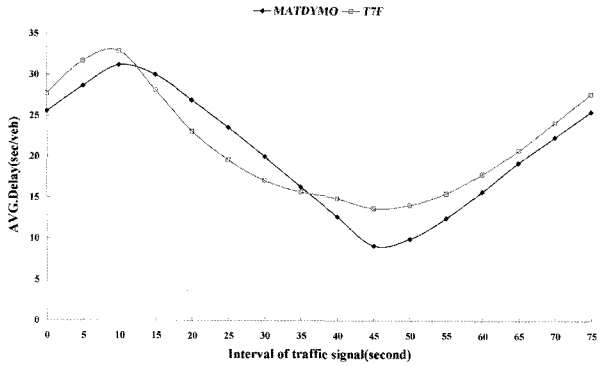

Figure 17. Variation of the average density by the interval of the traffic signals at 0.58 traffic volume.

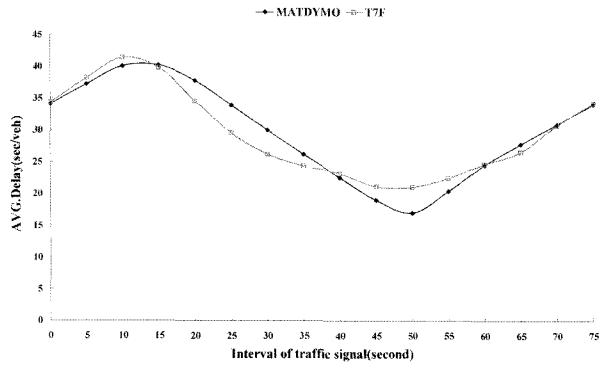

Figure 18. Variation of the average density by the interval of the traffic signals at 0.81 traffic volume.

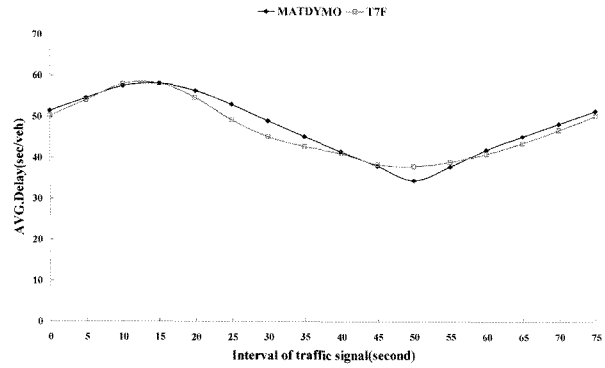

Figure 19. Variation of the average density by the interval of the traffic signals at 0.92 traffic volume.

25% at node 3. The applied vehicle acceleration rate ranged from -3 m/s^2~2.0 m/s^2. The average delay of node C was observed to be the same as that in the preceding simulation. The average traffic volume of road C was 0.71 in this simulation. Simulation was executed according to the interval of traffic signals between nodes 3 and 6, which varied from 0 to 75 s by 5s, and according to the traffic volume at road C, which was set to 0.58, 0.81, and 91. The simulation results were compared to those of TRANSYT-7F and this comparison is shown in Figures 17, 18, and 19.

As in the previous case, the MATDYMO gave very similar results to those of T7F for the variation of traffic volume. Regardless of the traffic volume, the maximum and minimum average delays were at the same interval of the traffic signals. The larger the traffic volume, the more the average delay increased. Because the road length was constant, the traffic volume increase meant increase of passing traffic volume per unit time. Therefore, if the traffic volume is large, the traffic signal must be controlled to mitigate traffic congestion and maintain continuous traffic flow.

5. CONCULSIONS

This paper presents our approach for building a multi-agent system in the traffic simulation, that is, the MATDYMO (Multi-Agent for Traffic Simulation with Vehicle Dynamic Model) system. The MATDYMO is constructed with four object-oriented sub systems. The sub systems of the MATDYMO are road management system, the vehicle motion control system, the driver management system, and the integration control system.

The driver is built as an agent to represent the diversity of the driver and to make a decision about the path finding. The Driver agent contains the physical attributes of the driver's characteristics, such as carefulness and aggressive. It also includes the car-following and lane-changing behavior. The vehicle agent can express the microscopic vehicle behavior. Unlike in other research, the vehicle agent in this paper represents the physical vehicle itself represented by vehicle dynamics.

The simulation using MATDYMO was performed for an interrupted flow model. By the analysis of the agents' behaviors in the interrupted flow model, it is confirmed that an agent's behavior through every rules and communication frameworks could characterize the diversity of human behavior and vehicle well. The driving conditions of each vehicle were substantially affected by its adjacent agents. The change of traffic flow according to the interval of the traffic signals was investigated for an interrupted flow model. The results were compared with those from the commercial software, TRANSYT-7F.

The MATDYMO showed very similar result to T7F for all investigated cases. When the acceleration rate increased, the average delay changed more sensitively. Because the input traffic volume was constant, and if the acceleration rate increases, the passing traffic volume per unit time increases. Also, the larger the traffic volume, the more increase the average delay. Because the road length was constant, the increasing of traffic volume meant the increasing of passing traffic volume per unit

time. The result of interrupted flow model showed that the change of the traffic state was closely related with the interval of the traffic signals. For an interrupted flow model, the adequate interval control of traffic signals between intersections is needed to relieve the traffic congestion. The simulations confirmed that MATDYMO could represent the real traffic condition of an interrupted flow model. At the current stage of development, MATDYMO shows great promise and has significant implications for future traffic state forecasting research.

ACKNOWLEDGEMENT–This work was supported by the Postdoctoral Research Program of Sungkyunkwan University (2005).

REFERENCES

Ben-Akiva, M., Hirsh, M. and Prashker, J. N. (1985). Probabilistic and economic factors in highway geometric design: a climbing lane example. *Transportation Science* **19**, **1**, 38–57.

Cho, K. Y., Kwon, S. J. and Suh, M. W. (2005). Vehicle dynamics approach to multi-agent for traffic simulation I: development of traffic environment. *Int. J. Automotive Technology* **7**, **1**, 25–34.

Fujioka, T. and Suzuki, K. (1994). Control of longitudinal and lateral platoon using sliding control. *Vehicle System Dynamics* **23**, **8**, 647–664.

Helbing, D. and Schreckenberg, M. (1999). Cellular automata simulating experimental properties of traffic flow. *Physical Review,* **E59**, R2505–R2508.

International Standard. (2002). *Transport Information and Control Systems - Adaptive Cruise Control Systems - Performance Requirements and Test Procedures.* ISO 15622.

Jones, G. E. (1993). Knowledge-based systems for crop protection: theory and practice. *Crop Protection* **12**, **8**, 565–578.

Kuri, J., Puech, N., Gagnaire, M. and Dotaro, E. (2002). Routing foreseeable lightpath demands using a tabu search meta-heuristic. *Global Telecommunications Conf.*, 2803–2807.

Kwon, S. J., Jang, S., Yoon, K. W. and Suh, M. W. (2004). A study on the VR simulation of the adaptive cruise controlled Vehicles. *J. Korean Society of Automotive Engineers* **12**, **4**, 632–638.

Lin, M. T. and Gan, A. C. (1999). Signal timing optimization for oversaturated networks using TRANSYT-7F. *Transportation Research Record,* **1683**, 118–126.

Mataric, M. (1994). *Interaction and Intelligent Behavior.* Technical Report AI-TR-1495. MIT Artificial Intelligence Lab.

Nakamiti, G. and Freitas, R. (2002). Adaptive, Real-time traffic control management. *Int. J. Automotive Technology* **3**, **3**, 89–94.

Reynolds, C. W. (1987). Flocks, Herds, and Schools: A distributed behavioral model. *Computer Graphics: Proc. SIGGRAPH '87* **21**, **4**.

Venhovens, P. Naab, K. and Adiprasito, B. (2000). Sop and go cruise control. *Int. J. Automotive Technology* **1**, **2**, 61–69.

Wenpin, J. and Hong, M. (2004). Automated adaptations to dynamic software architectures by using autonomous agents. *Engineering Applications of Artificial Intelligence* **17**, **7**, 749–770.